

FTIR Microscopic Imaging of Large Samples with 4x and 15x Infrared Objectives: A Case Study of a Carcinoma Tissue Section

Application note

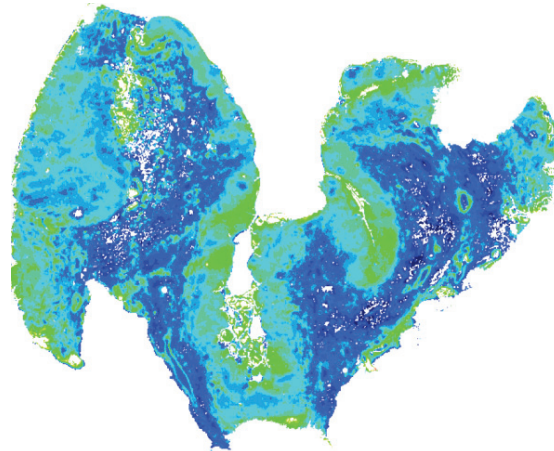
Biomedical Research

Author

Claudia Beleites*, Jürgen Popp*,
Christoph Krafft*, Mustafa Kansiz†

* Institute of Photonic Technology,
Albert-Einstein-Str. 9, 07745 Jena,
Germany

† Agilent Technologies, Australia
Pty. Ltd.



Introduction

Fourier transform infrared (FTIR) microscopic imaging uses a combination of an FTIR spectrometer with a microscope and Focal Plane Array (FPA) detector. The method has been recognized as a powerful and versatile imaging tool. The Field Of View (FOV) depends on both the magnification of the objectives, other magnification elements and the detector size. Agilent offers a proprietary IR objective with 4x magnification to substantially increase the FOV.



Agilent Technologies

Using typical IR microscope objectives with 15x magnification and a FPA with 64×64 pixels, the FOV in the Agilent 620 FTIR microscope is 350×350 μm and each pixel corresponds to an area of 5.5×5.5 μm in the sample plane. Larger FOVs can be realized in several ways:

- Using Agilent’s unique 4x IR objective to increase the FOV to provide up to 2.4x2.4 mm in a single tile using a 128x128 FPA.
- Larger FPAs of 128×128 pixels can be installed to image a FOV of 700×700 μm while maintaining the pixel size at 5.5×5.5 μm with the standard 15x objective.
- A mosaic of sequentially collected FTIR images can be composed to one image with a user-selected FOV.

The current application note presents data comparing mosaics that were obtained from a carcinoma tissue section using the new 4x IR and the standard 15x IR objectives. This practical study demonstrates how hardware flexibility can provide a range of collection conditions so that users can tailor their setup for a particular sample system. It also provides examples of where and how to use the 4x objective.

Data file size considerations

The Agilent Cary 620 FTIR microscope was coupled to an Agilent Cary 670 FTIR spectrometer (Figure 1). All data was collected at 4 cm⁻¹ spectral resolution, with 16 co-added scans for the sample measurement and 32 co-added scans for the background measurement (through an empty CaF₂ slide). The measurement parameters are summarized in Table 1 and the FPA tile mosaic configurations are shown in Figure 2. The attenuator and integration times were optimized to achieve the highest possible integration time before the onset of non-linear behavior, as determined by a “non-zero” detector response below the FPA spectral cutoff.

An under-sampling (UDR) scan setting of 4 was used, which limits the Fourier transform computed spectra up to 3975 cm⁻¹. To avoid aliasing from spectral contribution beyond 3975 cm⁻¹, a low pass optical filter was employed with a cut-off at approximately 3975 cm⁻¹.

Stage parameters for step size and offset were set for optimum stitching of images during mosaic acquisition. The values for step size also represent the FOV of a single FPA tile. The nominal pixel size was calculated by dividing the FOV by 64, which is the size



Figure 1. Agilent Cary 620 FTIR microscope coupled with an Agilent 670 FTIR spectrometer for FTIR microscopic imaging

of the FPA. All single beam spectra of an empty CaF_2 slide in transmission mode show maximum intensity near 1300 cm^{-1} and a strong decrease towards lower wavenumbers. The cutoff is at approximately 850 cm^{-1} for the 15x objective and 1000 cm^{-1} for the 4x objective. The better transmission of the 15x objective is due to the all-reflective Cassegrain geometry, whereas the transmission of the 4x objective is reduced in the low wavenumber range by lenses made of CaF_2 .

Table 1. Measurement parameters. All mosaics were collected with the same scan parameters: 16 co-additions for the scan, 32 co-additions for background, 4 cm^{-1} spectral resolution.

| Objective | 4x | 15x |
|---------------------------------------|-----------|---------|
| Integration time (μs) | 12 | 8 |
| Attenuation setting | Open | Open |
| Single FPA tile FOV (μm) | 1230x1230 | 350x350 |
| Nominal pixel size (μm) | 19.2x19.2 | 5.5x5.5 |
| Mosaic config. | 7x6 | 27x19 |
| Total mosaic size (mm) | 8.6x7.4 | 8.4x6.7 |
| Disk usage (GB) | 4.3 | 42.4 |
| Collection time (hh:mm) | 1:03 | 10:22 |

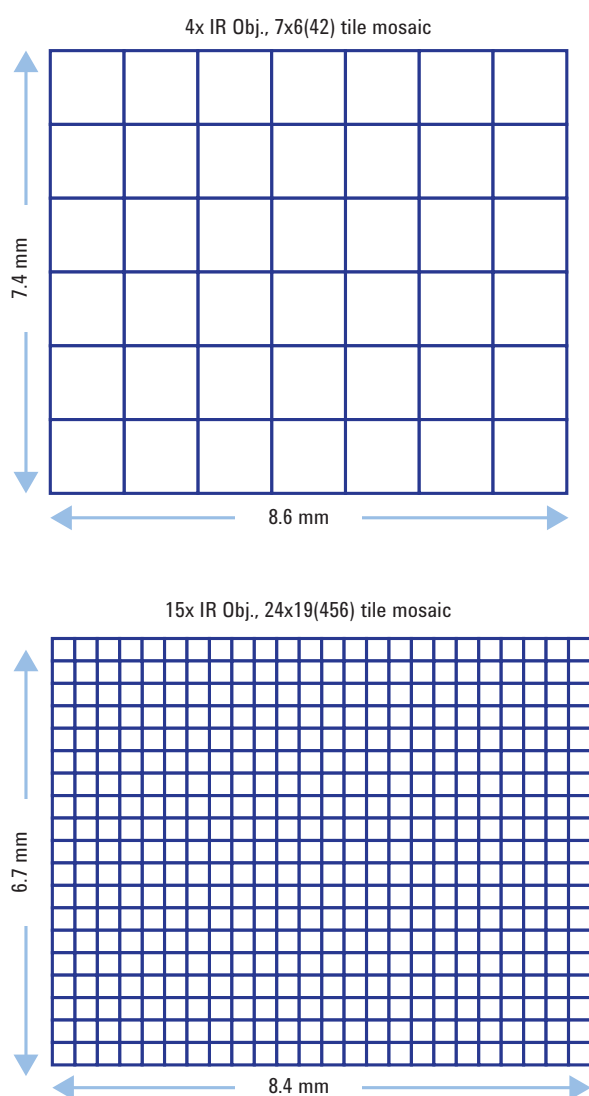


Figure 2. FPA tile mosaic configurations as per Table 1.

The size of the carcinoma tissue section that was prepared on a CaF_2 slide was approximately $8\times 6\text{ mm}$ (Figure 3).

As a consequence of the differences in FOVs, the mosaic FPA tile configuration ranged from from 7x6 to 24x19 giving total data sizes from 4.3 GB to 42.4 GB and total collection times from 1 hour to 10.5 hours for a collection area of up to $8.6\times 7.4\text{ mm}$. Collection times can be further reduced by a factor approximately 4x if a larger FPA detector (with its larger FOV) were used, such as a 128x128. Each FTIR image was stored as a separate file using the unique “multifile” data collection option of the Agilent Resolution Pro software. The advantage of this option is that mosaics of virtually unlimited size can be collected.

Data processing considerations

The size of the data sets was a challenge for data processing as is briefly described below. An external cluster server (MFS5520VIBR Board, 1xIntel Xeon Six-Core X5660 S1366, 2.8 GHz Processor, 8GB Dual-Kit DDR3-RAM 1066 MHz) under the operating system Linux was used. The data was imported into the “R” software package using the toolbox “hyperSpec”. FTIR spectra with a negative quality test were removed from the data set. These pixels include spectra with low signal intensities outside the specimen, and spectra with high spectral contributions from embedding media.

The total spectral integrated intensities of the FTIR image were plotted in Figure 3 where the removed spectra are represented by white.

As the high wavenumber range from 2800 to 3150 cm^{-1} did not significantly contribute to the distinction of tissue classes, it was not considered further. An alternative way to reduce the size of the data set is a procedure called "binning" that averages a defined number of neighboring pixels to one pixel at the expense of the spatial resolution, but with the

advantage of increased signal-to-noise ratio (SNR). However, this procedure was not applied here.

Another approach to limiting file sizes is to employ further "under-sampling (UDR)" in the collection conditions. For example, the UDR 4 setting used in this study could be increased to UDR 8, allowing a spectral range up to 1975 cm^{-1} (with an appropriate low pass optical filter to prevent aliasing). This would further reduce the total data size by half, and would speed up processing. Finally, the spectra were baseline corrected

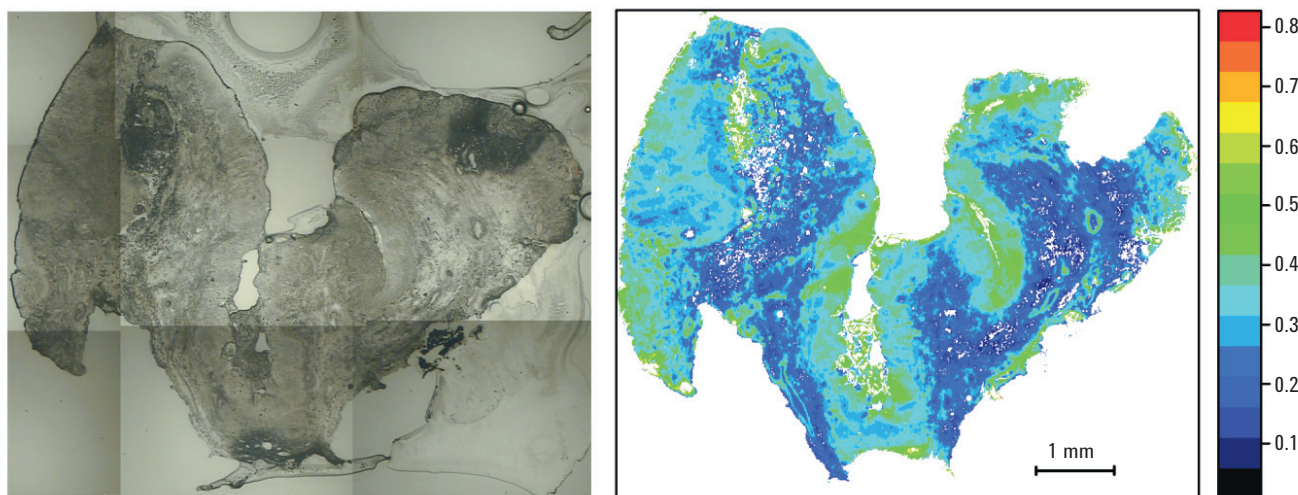


Figure 3. Left: Photomicrograph and FTIR image of unstained laryngeal carcinoma tissue section. Right: The total spectral intensity is plotted after pre-processing as described in the text.

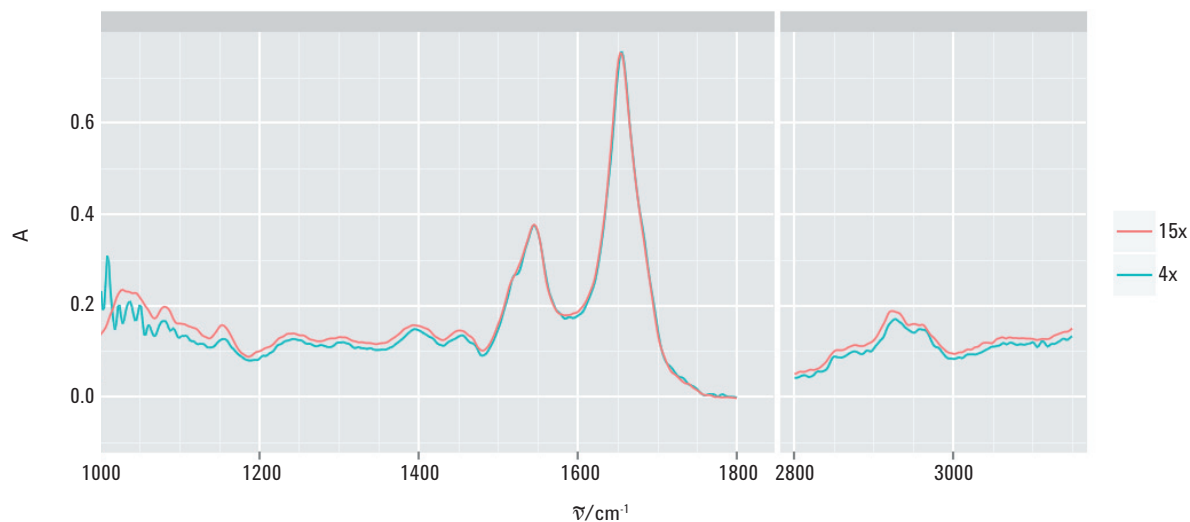


Figure 4. Overlay of FTIR spectra from carcinoma tissue section in the low and high wavenumber region comparing the following configurations: 15x and 4x objective.

and normalized. The overlay of spectra in Figure 4 shows that all spectra agree well at the position 5500, 2500 μm . According to the histopathologic inspection of a hematoxylin and eosin stained parallel tissue section (similar to that used in this FTIR imaging study), five classes can be identified: normal epithelium, connective tissue, inflammation, dysplasia, and carcinoma that co-localizes with blood and blood vessels. FTIR spectra representing each class were selected from the data set obtained by the 4x objective. These data trained a linear discriminant analysis (LDA) as classifier using the toolbox "cbmodel". This LDA model was applied to assign the FTIR spectra for the 15x data set after preprocessing. Figure 5 shows the results for the full tissue section and Figure 6 for a region of interest.

Comparison of images

The assignments of the spectra to one of the five tissue classes are shown in a green color scale. Overall, the

assignments are similar for the full specimen (Figure 5). Two small areas in the left and middle portion are assigned to carcinoma and blood, and large areas in the left and right portion are assigned to connective tissue. Dysplasia was found adjacent to carcinoma, and inflammatory response co-localizes with dysplasia. Three small areas are attributed to epithelium as normal tissue from which dysplasia and carcinoma originate.

One of the normal tissue areas was selected for a detailed inspection (Figure 6). The distinction of the three main classes, connective tissue, dysplasia and normal tissue, agrees well for both objectives with and without field expansion. Deviations occur for the minor classes carcinoma/blood and inflammation. The different pixel sizes demonstrate spatial resolutions. Only at higher resolution near 5 μm with a 15x objective and without field expansion does the morphology indicate a blood vessel with an empty lumen.

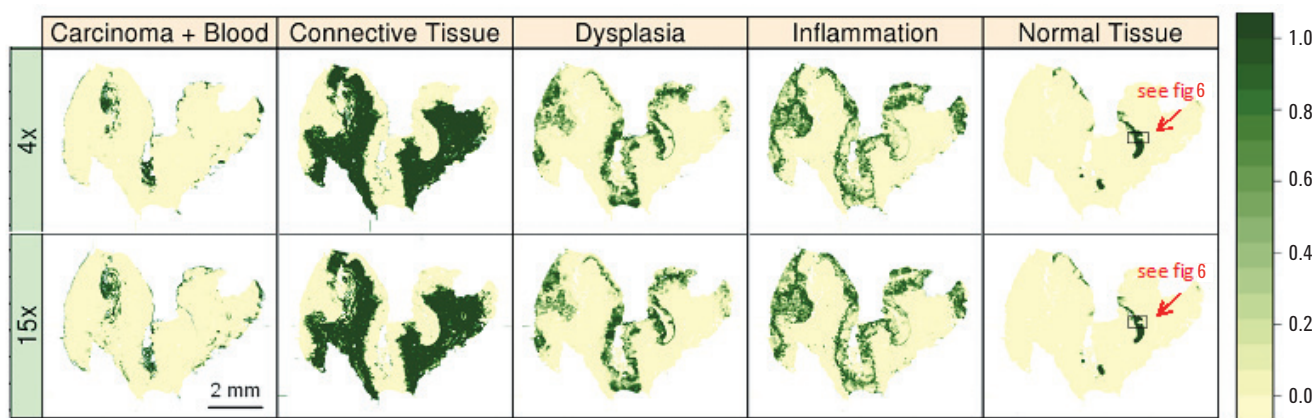


Figure 5. Discrimination of tissue types in full FTIR images by LDA classifier. The classifier was trained with selected spectra from an FTIR image collected with a 4x objective in the spectral range from 1200 to 1800 cm^{-1} . The soft classification was color-scaled from green to yellow. The boxes in the last column show the location of the region of interest shown in Figure 6.

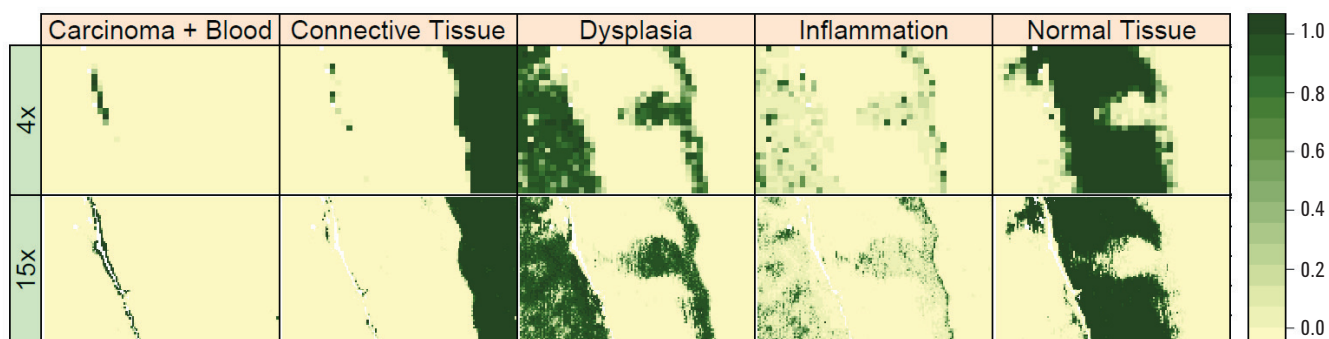


Figure 6: Discrimination of tissue types in the 750 μm x 500 μm region of interest to resolve details in the FTIR images shown in Figure 5.

Summary

A case study of a laryngeal carcinoma tissue section encompassing five tissue types was performed using an FTIR imaging microscope with 4x and 15x objectives. In terms of SNR and IR illumination uniformity, all configurations had similar, excellent quality. The questions were: how closely do the FTIR images compare, how is tissue discrimination expressed, and how does the pixel size affect what answers can be extracted from the data.

The benefits of larger FOV are clear in terms of data size and acquisition time, especially if mosaics are collected. According to Table 1, the FOV increases by a factor of $3.4 \times 3.4 \approx 11$. Therefore, the 4x objective is ideally suited for rapid survey scans. There are sample systems where $19 \mu\text{m}$ per pixel is enough to obtain useful data. In our case study, this holds true for defining margins between the main tissue types. The 15x objective with $5.5 \mu\text{m}$ per pixel was required to resolve details such as blood vessels. Furthermore, it is advisable to use the 15x rather than the 4x objective if the low wavenumber range below 1100 cm^{-1} contains important chemical information. For biochemically relevant samples, this includes cases such as:

- The symmetric phosphate vibration near 1080 cm^{-1} that is typical of phospholipids and nucleic acids.
- Glycogen, as representative of carbohydrates with bands near 1030 , 1080 and 1150 cm^{-1} .
- Cholesterol band near 1060 cm^{-1} .
- Hydroxyapatite as representative of mineralized tissue with a band near 1080 cm^{-1} .

For some molecules, equivalent bands in the wavenumber range above 1200 cm^{-1} are available, for example the antisymmetric phosphate vibration near 1235 cm^{-1} . Overall, the set of two 4x IR objectives—one as condenser and one as objective—is an excellent complement to the standard set of 15x objectives for FTIR imaging. For samples on reflective slides (e.g. MirrIR from KevleyTechnologies), one objective is sufficient in transfection geometry.

Acknowledgements

This research is supported within the European program EFRE (Europäischer Fonds für regionale Entwicklung, FKZ B714-07037 and B715-07038).

www.agilent.com

For Research Use Only. Not for use in diagnostic procedures.

Agilent shall not be liable for errors contained herein or for incidental or consequential damages in connection with the finishing, performance or use of this material.

Information, descriptions, and specifications in this publication are subject to change without notice.

© Agilent Technologies, Inc. 2014

Published October 16, 2014

Publication number: 5991-1363EN



Agilent Technologies